Noname manuscript No.
(will be inserted by the editor)

Numerical Evaluation of Mittag-Leffler Functions

William McLean

arXiv:2208.03851v1 [math.NA] 8 Aug 2022

August 9, 2022

Abstract The Mittag-Leffler function is computed via a quadrature approximation of a contour integral representation. We compare results for parabolic and hyperbolic contours, and give special attention to evaluation on the real line. The main point of difference with respect to similar approaches from the literature is the way that poles in the integrand are handled. Rational approximation of the Mittag-Leffler function on the negative real axis is also discussed.

Keywords Special functions · Fractional calculus · Quadrature · Contour integration · Rational approximation

Mathematics Subject Classification (2010) 33F05 · 41A20 · 65D32

1 Introduction

The Mittag-Leffler function [5, 13] is defined by the power series

$$E_\alpha(z) = \sum_{n=0}^{\infty} \frac{z^n}{\Gamma(1+n\alpha)}, \tag{1}$$

which converges for all $z \in \mathbb{C}$ if $\alpha > 0$. For integer values of α we can express E_α in terms of elementary functions [15, Equation (1.5)], e.g.,

$$E_0(z) = \frac{1}{1-z}, \qquad E_1(z) = e^z, \qquad E_2(z) = \cosh(z^{1/2}) = \sum_{n=0}^{\infty} \frac{z^n}{(2n)!}, \tag{2}$$

and for $\alpha = 1/2$ in terms of the scaled complementary error function [7, Equation (2.7)],

$$E_{1/2}(z) = \operatorname{erfcx}(-z) \quad \text{where} \quad \operatorname{erfcx}(z) = \frac{2}{\sqrt{\pi}} \int_z^\infty \exp(z^2 - t^2)\, dt.$$

Numerical evaluation of the series (1) is efficient for small $|z|$, but other approaches are required in general.

William McLean
School of Mathematics and Statistics, University of New South Wales, Sydney 2052, Australia
E-mail: w.mclean@unsw.edu.au

The Mittag–Leffler function has been mostly neglected by those responsible for mathematical software libraries, apparently because until the 1990s there were few applications that called for numerical values of $E_\alpha(z)$. Mathematica seems to provide the only officially supported implementation with its `MittagLefflerE` function. Growing interest in the applications of fractional calculus, such as in fractional partial differential equation models, led in the 2000s to a growing demand for methods to evaluate $E_\alpha(z)$, particularly for the case $0 < \alpha < 1$ with z on the negative real axis. Such applications involve also the two-parameter Mittag-Leffler function,

$$E_{\alpha,\beta}(z) = \sum_{n=0}^{\infty} \frac{z^n}{\Gamma(\beta + n\alpha)}, \tag{3}$$

as well as other generalizations beyond the scope of this paper. The identity [7, Equation (5.4)]

$$\frac{d}{dz} E_{\alpha,\beta}(z) = \frac{1}{\alpha z}\bigl[E_{\alpha,\beta-1}(z) - (\beta-1)E_{\alpha,\beta}(z)\bigr]$$

means that if the Mittag-Leffler function can be evaluated then so can its derivative.

Gorenflo et al. [6] and Seybold and Hilfer [18] developed methods to compute $E_{\alpha,\beta}(x)$ based on contour integral representations and asymptotic expansions for large $|z|$. These authors provide computable error bounds that reduce the problem to evaluating integrals of complex-valued functions defined on finite real intervals, which then require some kind of numerical quadrature. Igor Podlubny [17] wrote a widely used, third-party Matlab function, `mlf`, based on these methods.

Weideman and Trefethen [19] developed a quadrature method for numerical inversion of the Laplace transform via the Bromich integral formula, thereby providing another way to evaluate E_α. The method was developed further by Garrappa [2,3] who contributed another third-party Matlab code, `ml`. Gill and Straka [4] used a similar approach in their R package, `MittagLeffleR`, which handles Mittag-Leffler probability distributions.

The approach used here is similar to that of Garrappa [2], but whereas he used the contour integral representation

$$e_{\alpha,\beta}(t;\lambda) = t^{\beta-1}E_{\alpha,\beta}(t^\alpha\lambda) = \frac{1}{2\pi i}\int_{\mathscr{C}} e^{st}\,\frac{s^{\alpha-\beta}\,ds}{s^\alpha - \lambda}, \quad t > 0, \quad \lambda \in \mathbb{C}, \tag{4}$$

we will work with the Wiman integral,

$$E_{\alpha,\beta}(z) = \frac{1}{2\pi i}\int_{\mathscr{C}} \frac{e^w w^{\alpha-\beta}}{w^\alpha - z}\,dw. \tag{5}$$

In both cases, one makes a branch cut along the negative real axis (in the s-plane and w-plane respectively) and chooses a Hankel contour $\mathscr{C}$ that encircles this cut in the counterclockwise direction, beginning at infinity in the third quadrant, passing to the right of all singularities in the integrand, and finishing at infinity in the second quadrant. The two representations are related via the substitution $w = st$.

When applying the method of Weideman and Trefethen to evaluate (4), the contour $\mathscr{C}$ is chosen to be a parabola or hyperbola that depends on t. The parameters describing this contour, together with the step size in the quadrature formula, are chosen to optimize the convergence rate. We use essentially the same approach for (5) but with a fixed $\mathscr{C}$ independent of z. The more substantial difference in our approach concerns the treatment of any poles that arise when the denominator of the integrand vanishes. Whereas Garrappa avoids

the poles by adjusting $\mathscr{C}$, we instead split the integrand into a simple singular term and a remainder that is analytic in the cut plane.

After summarizing a few standard properties of the Mittag-Leffler function in Section 2, we present the quadrature method in Section 3. If the argument z is real, then the computational cost of the method can be reduced using techniques we describe in Section 4. For comparison, Section 5 considers rational approximations of Padé type that were introduced by Zeng and Chen [21]. Finally, in Section 6 we present some numerical examples of minimax approximation of $E_\alpha(-x)$ for $0 \le x < \infty$ using rational functions of type (m,m).

A Julia package [11] implements the numerical methods described herein. The scripts used to generate the figures and tables below are included in the `examples` folder of the package repository on Github. All computations were performed in 64-bit floating point arithmetic although some routines in the package support the use of Julia's `BigFloat` multiple precision data type.

2 Integral representation and asymptotics

Properties of the Mittag-Leffler function are described at length in the survey article of Haubold et al. [7] and the mongraph of Gorenflo et al. [5]. We will require only a few simple facts that are easily derived using the integral representation of the reciprocal of the Gamma function:

$$\frac{1}{\Gamma(\nu)} = \frac{1}{2\pi i}\int_{\mathscr{C}} \frac{e^w}{w^\nu}\,dw. \tag{6}$$

By choosing $\mathscr{C}$ so that it passes to the right of the circle $|w| = |z|^{1/\alpha}$, as illustrated in Fig. 1, and using (6) with $\nu = \beta + n\alpha$ in (3), the integral representation (5) follows by summation of a geometric series, which converges because $|z/w^\alpha| < 1$ for all $w \in \mathscr{C}$.

Suppose now that $0 < \alpha < 1$ and $z \neq 0$ with $\theta = \arg z \in (-\pi,\pi]$. If $\alpha\pi < |\theta| < \pi$, then $w^\alpha - z \neq 0$ for w in the cut plane $|\arg w| < \pi$ and we find that $E_{\alpha,\beta}(z) = O(|z|^{-1})$ as $|z| \to \infty$. However, if $|\theta| < \alpha\pi$ then the equation $w^\alpha - z = 0$ has a single solution in the cut plane, namely $w = \gamma$ where

$$\gamma = z^{1/\alpha} = |z|^{1/\alpha}\exp(i\theta/\alpha). \tag{7}$$

Shifting the contour so it passes to the left of the pole at γ we collect a residue, with the result that

$$E_{\alpha,\beta}(z) = \alpha^{-1}\gamma^{1-\beta}\exp(\gamma) + \frac{1}{2\pi i}\int_{\mathscr{C}'} \frac{e^w w^{\alpha-\beta}}{w^\alpha - z}\,dw, \tag{8}$$

and the integral over the shifted contour $\mathscr{C}'$ is again $O(|z|^{-1})$ as $|z| \to \infty$.

The identity

$$E_{\alpha,\beta-\alpha}(z) = \frac{1}{\Gamma(\beta-\alpha)} + zE_{\alpha,\beta}(z) \tag{9}$$

follows easily from the power series (3), leading to the asymptotic formulae

$$\begin{aligned} E_{\alpha,\beta}(z) &= \frac{-z}{\Gamma(\beta-\alpha)} + z^{-1}E_{\alpha,\beta-\alpha}(z) \\ &= -\frac{z^{-1}}{\Gamma(\beta-\alpha)} + \begin{cases} O(|z|^{-2}) & \text{if } \alpha\pi < |\theta| \le \pi, \\ \alpha^{-1}z^{(1-\beta)/\alpha}\exp(z^{1/\alpha}) + O(|z|^{-2}) & \text{if } |\theta| < \alpha\pi, \end{cases} \end{aligned}$$

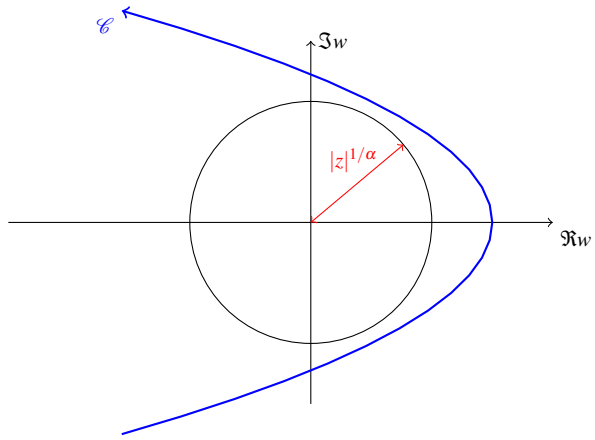

Fig. 1 The Hankel contour $\mathscr{C}$.

Iterating this result, we find that [16, Equation (1.2)]

$$E_{\alpha,\beta}(z) = -\sum_{n=1}^{m-1} \frac{z^{-n}}{\Gamma(\beta-n\alpha)} + \begin{cases} O(|z|^{-m}) & \text{if } \alpha\pi < |\theta| \le \pi, \\ \alpha^{-1} z^{(1-\beta)/\alpha} \exp(z^{1/\alpha}) + O(|z|^{-m}) & \text{if } |\theta| < \alpha\pi, \end{cases} \tag{10}$$

The behaviour around the Stokes lines $\theta = \pm\alpha\pi$ is quite subtle and has been studied in detail by Paris [16, 15] and by Wong and Zhao [20].

Example 2.1 Since $|\exp(z^{1/\alpha})| = \exp(|z|^{1/\alpha}\cos\theta/\alpha)$ and $\cos\theta/\alpha > 0$ for $|\theta| < \alpha\pi/2$, it follows that in this sector $E_{\alpha,\beta}(z)$ exhibits super exponential growth. This behaviour can be seen, for $\alpha = 3/4$, in Fig. 2, which shows a contour plot of $\log_{10}|E_{3/4}(z)|$ for $-6 \le \Re z \le 2$ and $-4 \le \Im z \le 4$. Notice the zeros near $\pm 3{\cdot}7i$.

Remark 2.1 When $|z|$ is sufficiently large, dropping the $O(|z|^{-m})$ remainder term from the asymptotic formula (10) yields a practical numerical approximation $E_{\alpha,\beta}(z) \approx E^{\text{asymp}}_{\alpha,\beta,m}(z)$. Recalling the identity

$$\Gamma(z)\Gamma(1-z) = \frac{\pi}{\sin \pi z}, \tag{11}$$

we write the coefficient in the nth term of the asymptotic sum as $1/\Gamma(\beta-n\alpha) = \sigma_n\tau_n$ where

$$\sigma_n = 1 \quad \text{and} \quad \tau_n = \frac{1}{\Gamma(\beta-n\alpha)} \quad \text{if } n\alpha < \beta,$$

with

$$\sigma_n = -\sin\pi(n\alpha-\beta) \quad \text{and} \quad \tau_n = \frac{1}{\pi}\Gamma(1+n\alpha-\beta) \quad \text{if } n\alpha \ge \beta.$$

The accuracy of $E^{\text{asymp}}_{\alpha,\beta,m}(z)$ will improve with increasing m until $m \approx \alpha^{-1}|z|^{1/\alpha}$ [15, Section 2], after which the asymptotic sum begins to diverge. Thus, for a given error tolerance tol, a simple heuristic is to keep adding terms until $\tau_n|z|^{-n} < \text{tol}$ or $n > \alpha^{-1}|z|^{1/\alpha}$. If the former occurs first, then we can expect to achieve the desired accuracy; in either case, the size of $\tau_{m-1}|z|^{-(m-1)}$ should give an indication of the error. For a more rigorous approach to estimating the remainder in the asymptotic expansion, see Seybold and Hilfer [18, Theorem 4.2].

Table 1 Results approximating $E_{\alpha,\beta}(-x)$ by applying the algorithm of Remark 2.1, based on the asymptotic expansion (10), when $\alpha = 0.7$, $\beta = 1.0$ and tol $= 10^{-12}$.

x	m	$\alpha^{-1}x^{1/\alpha}$	Error	$\tau_{m-1}\lvert z\rvert^{-(m-1)}$	$\tau_m\lvert z\rvert^{-m}$
5	15	14.2	5.84e-06	1.21e-05	1.18e-05
15	16	68.4	8.11e-14	8.24e-13	2.82e-13
25	12	141.9	-6.54e-14	3.70e-13	6.09e-14
35	10	229.5	-1.25e-14	8.15e-13	8.31e-14
45	10	328.6	-4.09e-15	8.49e-14	6.73e-15
55	9	437.7	8.24e-15	2.34e-13	1.39e-14

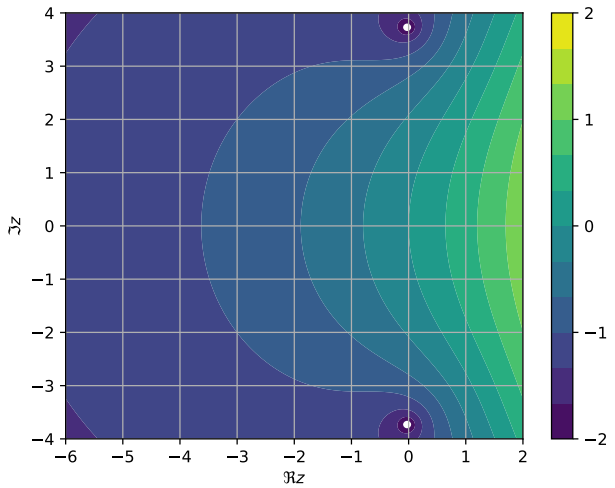

Fig. 2 Contour plot of $\log_{10}|E_{3/4}(z)|$.

Example 2.2 Let $z = -x$ for $x > 0$ and consider the error $E_{\alpha,\beta}(-x) - E^{\text{asymp}}_{\alpha,\beta,m}(-x)$. Table 1 shows some results applying the method of Remark 2.1 with $\alpha = 0.7$, $\beta = 1$ and tol $= 10^{-12}$. We see that for $x = 5$ the asymptotic series is at best accurate only to about 5 decimal places, but for all other cases the error is smaller than tol for values of m that are much smaller than $\alpha^{-1}x^{1/\alpha}$. In all cases, the error is smaller than $\tau_{m-1}x^{-(m-1)}$.

For $\alpha > 1$, the equation $w^\alpha - z = 0$ possesses more solutions with $|\arg w| \le \pi$, complicating the behaviour of $E_{\alpha,\beta}(z)$. Fortunately, once we are able to evaluate the Mittag-Leffler function for $0 < \alpha \le 1$, we can handle the case $\alpha > 1$ using the identity [7, Equation (3.8)]

$$E_{\alpha,\beta}(z) = \frac{1}{m}\sum_{k=0}^{m-1} E_{\alpha/m,\beta}\left(z^{1/m}e^{i2\pi k/m}\right) \quad \text{for } m \in \{1,2,3,\ldots\}, \tag{12}$$

by choosing m to be the unique integer satisfying $m-1 < \alpha \le m$, so that $0 < \alpha/m \le 1$.

3 Quadrature method

We now consider the numerical evaluation of the integral

$$E_{\alpha,\beta}(z) = \frac{1}{2\pi i}\int_{\mathscr{C}} e^w f(w;z)\,dw \quad \text{where} \quad f(w;z) = \frac{w^{\alpha-\beta}}{w^\alpha - z}, \tag{13}$$

assuming $0<\alpha<1$ and, to begin with, $\alpha\pi < |\theta| \le \pi$ so $f(w;z)$ is analytic for all w in the cut plane.

3.1 Parabolic contour

We adapt the approach of Weideman and Trefethen [19], who proposed a Hankel contour $\mathscr{C} = \{\, w(u) : -\infty < u < \infty \,\}$ where

$$w(u) = \mu(1+iu)^2 \quad \text{for } -\infty < u < \infty, \text{ with } \mu > 0. \tag{14}$$

Since

$$\Re w(u) = \mu(1-u^2) \quad \text{and} \quad \Im w(u) = 2\mu u, \tag{15}$$

we see that $\mathscr{C}$ is a parabola cutting the real axis at μ, with $\Re w(u) \to -\infty$ as $|u| \to \infty$. Write

$$\frac{1}{2\pi i}\int_{\mathscr{C}} e^w f(w;z)\,dw = \int_{-\infty}^{\infty} g(u;z)\,du \quad \text{where} \quad g(u;z) = \frac{e^{w(u)}}{2\pi i} f\big(w(u);z\big)w'(u) \tag{16}$$

and, for a suitable step size $h>0$, let us seek to approximate this integral by an infinite sum

$$Q_h(f;z) = h\sum_{n=-\infty}^{\infty} g(nh;z).$$

The error analysis for $Q_h(f;z)$ begins by extending the parametric representation (14) to a conformal mapping $\zeta = u+iv \mapsto w(u+iv) = \mu(1-v+iu)^2$. Since

$$\Re w(u+iv) = \mu\big((1-v)^2 - u^2\big) \quad \text{and} \quad \Im w(u+iv) = 2\mu(1-v)u,$$

we see that $u \mapsto w(u+iv)$ is again a parabola with $\Re w(u+iv) \to -\infty$ as $|u| \to \infty$. It is necessary to assume $v<1$ so that $\Im w(u+iv)$ is an increasing function of u. In fact, as v increases to 1 the parabola collapses onto the cut along the negative real axis. Thus, if $0<r<1$ and $s>0$, then $g(\zeta;z)$ is analytic on the strip $-s \le \Im\zeta \le r$ and we have the error bound [12, Theorem 5.2]

$$\left| Q_h(f,z) - \int_{-\infty}^{\infty} g(u;z)\,du \right| \le \frac{M(r;z)}{\exp(2\pi r/h)-1} + \frac{M(-s;z)}{\exp(2\pi s/h)-1}, \tag{17}$$

where $M(v;z) = \int_{-\infty}^{\infty} |g(u+iv;z)|\,du$.

In practice, we must truncate the infinite sum and compute, for some positive integer N,

$$Q_{h,N}(f;z) = h\sum_{n=-N}^{N} g(nh;z), \tag{18}$$

which, in view of (15), leads to an additional error of order $\exp\big(\mu(1-(Nh)^2)\big)$ from the sum over $|n| \ge N+1$. Putting $r = r_\delta = 1-\delta$, we have

$$M(r_\delta;z) \le C_\delta \exp\big(\mu\delta^2\big) \quad \text{and} \quad M(s;z) \le C_s \exp\big(\mu(1+s)^2\big),$$

and hence the overall quadrature error $\varepsilon_N = \varepsilon_N(\mu, r, s, h)$ is of order

$$\exp(\mu\delta^2 - 2\pi r_\delta/h) + \exp\big(\mu(1+s)^2 - 2\pi s/h\big) + \exp\big(\mu(1-(Nh)^2)\big).$$

Only the second term depends on s, so we minimise

$$\mu(1+s)^2 - \frac{2\pi s}{h} = \mu\left[\left(s+1-\frac{2\pi}{\mu h}\right)^2 + \frac{2\pi}{\mu h} - \left(\frac{\pi}{\mu h}\right)^2\right]$$

by choosing $s+1 = 2\pi/(\mu h)$. To balance the three error terms we then require

$$\mu\delta^2 - \frac{2\pi r_\delta}{h} = \frac{2\pi}{h} - \frac{\pi^2}{\mu h^2} = \mu\big(1-(Nh)^2\big).$$

Neglecting δ, the optimal parameters are $h_\star = 3N^{-1}$ and $\mu_\star = (\pi/12)N$, giving a quadrature error $\varepsilon_N(\mu_\star, h_\star)$ of order $\exp(-2\pi/h_\star) = \exp(-2\pi N/3) \approx 8{\cdot}12^{-N}$.

For this optimized choice of the parameters, we will denote the quadrature sum by

$$Q_{\star,N}(f;z) = Q_{h_\star,N}(f;z), \tag{19}$$

Since $w'(u) = 2\mu_\star i(1+iu)$ we have

$$\frac{h_\star w'(u)}{2\pi i} = \frac{\mu_\star h_\star}{\pi}(1+iu) = \frac{1+iu}{4}$$

so

$$Q_{\star,N}(f;z) = A\sum_{n=-N}^{N} C_n f\big(w(nh_\star);z\big) \tag{20}$$

where

$$A = \frac{1}{4} \quad \text{and} \quad C_n = e^{w(nh_\star)}(1+inh_\star). \tag{21}$$

The properties

$$w(-u) = \overline{w(u)} \quad \text{and} \quad C_{-n} = \overline{C}_n, \tag{22}$$

mean that it suffices to store the points $w(nh_\star)$ and coefficients C_n for $0 \le n \le N$. Note, however, that our notation hides the fact that $w(nh_\star)$ and C_n depend not only on n but also on N. Thus, increasing N means recomputing *all* of the points and coefficients.

Remark 3.1 The error analysis above implicitly assumes that the factor $e^{w(u)}$ dominates the influence of the integrand $g(u;z)$ in (16). On the one hand, since $f(w;z) = O(|w|^{\alpha-\beta})$ as $|w| \to 0$, we see that the factor $M(r;z)$ in the error bound (17) will grow for large positive β. On the other hand, since $f(w;z) = O(|w|^{-\beta})$ as $|w| \to \infty$, the factor $M(-s;z)$ will grow for large negative β. To alleviate the growth of $M(r;z)$, Garrappa and Popolizio [3, Section 3] modified the above approach by considering a restriction $r \le \text{const} < 1$, so that the parabola $u \mapsto w(u+ir)$ does not pass too close to the origin. An alternative is to reduce the value of β used in the quadrature approximation via the identity [7, Section 5]

$$E_{\alpha,\beta}(z) = z^{-m}E_{\alpha,\beta-m\alpha}(z) - \sum_{n=1}^{m}\frac{z^{-n}}{\Gamma(\beta-n\alpha)}.$$

Similarly, growth in $M(-s;z)$ for large negative β may be ameliorated via the identity

$$E_{\alpha,\beta}(z) = z^{m}E_{\alpha,\beta+m\alpha}(z) + \sum_{n=0}^{m-1}\frac{z^{n}}{\Gamma(\beta+n\alpha)}.$$

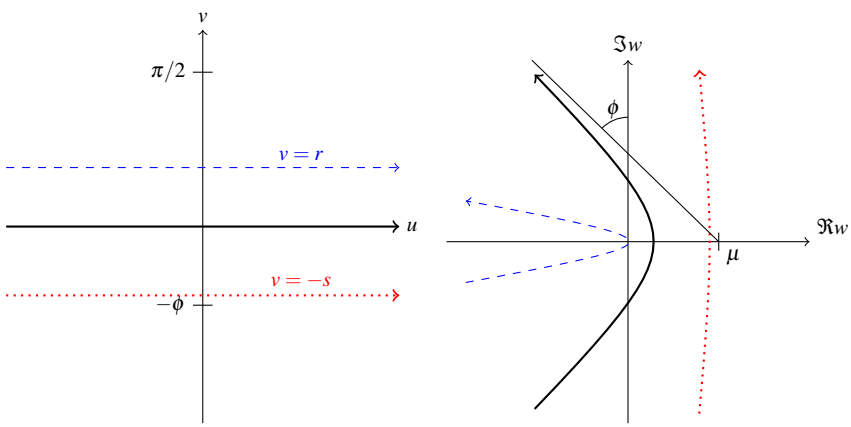

Fig. 3 Hyperbolas parameterised by $u \mapsto w(u+iv)$.

3.2 Hyperbolic contour

The second type of contour considered by Weideman and Trefethen [19] is of the form

$$w(u) = \mu\bigl(1+\sin(iu-\phi)\bigr) \quad \text{for } -\infty < u < \infty, \tag{23}$$

where the parameters μ and ϕ satisfy $\mu > 0$ and $0 < \phi < \pi/2$; see also López-Fernández and Palencia [9]. Since $\Re w = \mu(1-\cosh u \sin\phi)$ and $\Im w = \mu \sinh u \cos\phi$, we have

$$\left(\frac{\Re w - \mu}{\mu \sin\phi}\right)^2 - \left(\frac{\Im w}{\mu\cos\phi}\right)^2 = 1,$$

so $\mathscr{C}$ is the left branch of an hyperbola with asymptotes $\Im w = \pm(\Re w - \mu)\cot\phi$. We extend (23) to a conformal mapping $\zeta = u+iv \mapsto w(u+iv) = \mu\bigl[1+\sin(iu-(\phi+v))\bigr]$, and see that for a fixed v with $0 < \phi+v < \pi/2$ the curve $u \mapsto w(u+iv)$ is the left branch of an hyperbola with asymptotes $\Im w = \pm(\Re w - \mu)\cot(\phi+v)$, as illustrated in Fig. 3 for $v = r$, 0 and $-s$. Noting that

$$\Re w(u+iv) \le \mu\bigl(1-\sin(\phi+v)\bigr) \quad \text{for } -\infty < u < \infty,$$

it follows that the error bound (17) can be applied for $0 < r < \pi/2 - \phi$ and $0 < s < \phi$ with

$$M(r_\delta;x) \le C\exp\bigl(\mu(1-\cos\delta)\bigr) \quad \text{and} \quad M(-s_\delta;x) \le C\exp\bigl(\mu(1-\sin\delta)\bigr),$$

where $r_\delta = \pi/2 - \phi - \delta$ and $s_\delta = \phi - \delta$.

After truncating the infinite sum as before to obtain a practical quadrature approximation (18), the overall error $\varepsilon_N = \varepsilon_N(\mu,\phi,h,\delta)$ is of order

$$M(r_\delta;z)\exp(-2\pi r_\delta/h) + M(-s_\delta;z)\exp(-2\pi s_\delta/h) + \exp\bigl(\mu(1-\cosh(Nh)\sin\phi)\bigr).$$

We again seek to minimise the overall quadrature error by balancing these three terms. Neglecting δ leads to the equations

$$\frac{\pi(2\phi-\pi)}{h} = \mu - \frac{2\pi\phi}{h} = \mu\bigl(1-\cosh(Nh)\,\sin\phi\bigr),$$

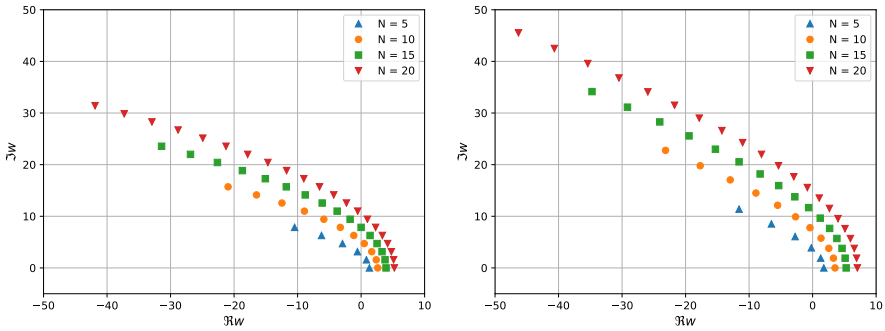

Fig. 4 The quadrature points $w(nh_\star)$ for $0 \le n \le N$ and four choices of N using parabolic (left) and hyperbolic (right) contours.

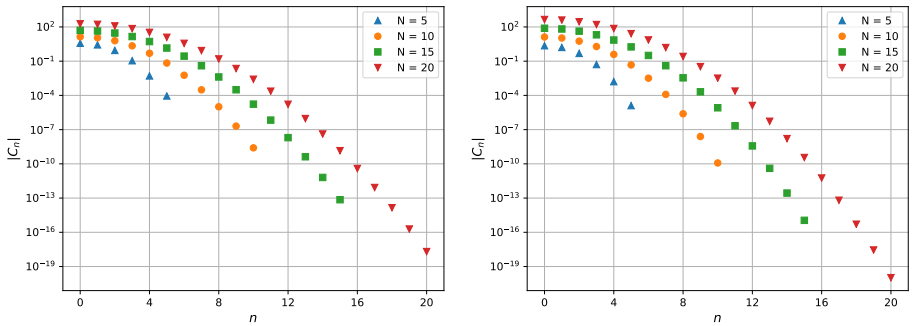

Fig. 5 The magnitudes $|C_n|$ of the complex weights for $0 \le n \le N$ and four choices of N using parabolic (left) and hyperbolic (right) contours.

which imply that

$$\mu = \frac{\pi(4\phi - \pi)}{h} \quad \text{and} \quad \cosh(Nh) = \frac{2\phi}{(4\phi - \pi)\sin\phi}.$$

In this way,

$$\mu = \frac{\pi(4\phi - \pi)}{a(\phi)} N \quad \text{and} \quad h = \frac{a(\phi)}{N} \tag{24}$$

where

$$a(\phi) = \operatorname{arcosh}\left(\frac{2\phi}{(4\phi - \pi)\sin\phi}\right) \quad \text{for } \frac{\pi}{4} < \phi < \frac{\pi}{2},$$

and with these choices of $\mu = \mu_N(\phi)$ and $h = h_N(\phi)$ the quadrature error satisfies

$$\varepsilon_N(\phi) = O\big(\exp(-b(\phi)N)\big) \quad \text{with} \quad b(\phi) = \frac{\pi(\pi - 2\phi)}{a(\phi)}.$$

The function $b(\phi)$ has a unique maximum value for $\phi \in [\pi/4, \pi/2]$ when $\phi = \phi_\star \doteq 1{\cdot}17210$, so $\varepsilon_N(\phi_\star)$ is of order $\exp\big(-b(\phi_*)N\big) \approx 10.13^{-N}$, indicating somewhat faster convergence than for the parabolic contour. Taking $\phi = \phi_\star$ in (24) gives the optimized parameter values $\mu_\star \doteq 4{\cdot}49198 \times N$ and $h_\star \doteq 1{\cdot}08180/N$.

Recalling the form of g from (16), and noting that

$$\frac{h_\star w'(u)}{2\pi i} = \frac{\mu_\star h_\star}{2\pi}\cos(iu-\phi_\star) = \frac{4\phi_\star-\pi}{2}\cos(iu-\phi_\star),$$

we obtain once again a sum of the form (19) but now with

$$A = 2\phi_\star - \frac{\pi}{2} \quad \text{and} \quad C_n = e^{w(nh_\star)}\cos(inh_\star-\phi_\star). \tag{25}$$

The coefficients again satisfy (22) so it suffices to store $w(nh_\star)$ and C_n for $0 \le n \le N$.

Figure 4 compares the locations of the quadrature points $w(nh_\star)$ on the parabolic and hyperbolic contours in the complex plane, for four choices of N. The magnitudes $|C_n|$ of the correponding coefficients are compared in Fig. 5.

Remark 3.2 Recalling the form of $f(w;z)$ from (13), we see that (19) provides a rational approximation to the contour integral,

$$Q_{\star,N}(f;z) = \sum_{n=-N}^{N} \frac{R_n}{z-P_n},$$

with poles $P_n = w(nh_\star)^\alpha$ and associated residues $R_n = -AC_n w(nh_\star)^{\alpha-\beta}$. Of course, these poles all lie outside the sector $\alpha\pi < |\arg z| \le \pi$ where $Q_{\star,N}(f;z)$ is used.

3.3 Extending the method to handle a pole in the integrand

Still assuming $0<\alpha<1$, we suppose now that $|\theta| \le \alpha\pi$ and recall that $w^\alpha - z = 0$ when $w=\gamma$; see (7). Write

$$\frac{w^{\alpha-\beta}}{w^\alpha - z} = \frac{w^{\alpha-\beta}\rho(w;z)}{w-\gamma} \quad \text{where} \quad \rho(w;z) = \frac{w-\gamma}{w^\alpha - z},$$

and observe that $\rho(w;z)$ has a removable singularity at $w=\gamma$ with $\rho(\gamma;z) = \gamma^{1-\alpha}/\alpha$. We define

$$f_1(w;z) = \frac{w^{\alpha-\beta}\rho(w;z) - \gamma^{\alpha-\beta}\rho(\gamma;z)}{w-\gamma} = \frac{w^{\alpha-\beta}}{w^\alpha - z} - \frac{\alpha^{-1}\gamma^{1-\beta}}{w-\gamma}, \tag{26}$$

so that

$$f(w;z) = \frac{w^{\alpha-\beta}}{w^\alpha - z} = \frac{\alpha^{-1}\gamma^{1-\beta}}{w-\gamma} + f_1(w;z)$$

and hence by (13),

$$E_{\alpha,\beta}(z) = \alpha^{-1}\gamma^{1-\beta}\exp(\gamma) + \frac{1}{2\pi i}\int_{\mathscr{C}} e^w f_1(w;z)\,dw. \tag{27}$$

Since f_1 is analytic in the whole cut plane, we can deform $\mathscr{C}$ into a parabolic or hyperbolic contour of the type considered above, and use the corresponding quadrature sum $Q_{\star,N}(f_1;z)$ to approximate the integral. Note that $f_1(w;z)$ is not a rational function of z since $\gamma = z^{1/\alpha}$.

To avoid roundoff problems evaluating $f_1(w;z)$ when w is close to γ, let $\varepsilon = (w-\gamma)/\gamma$ so that $w = \gamma(1+\varepsilon)$, and define

$$\psi_{1,\alpha}(\varepsilon) = \frac{(1+\varepsilon)^\alpha - 1}{\varepsilon} = \sum_{k=1}^{\infty}\binom{\alpha}{k}\varepsilon^{k-1} \tag{28}$$

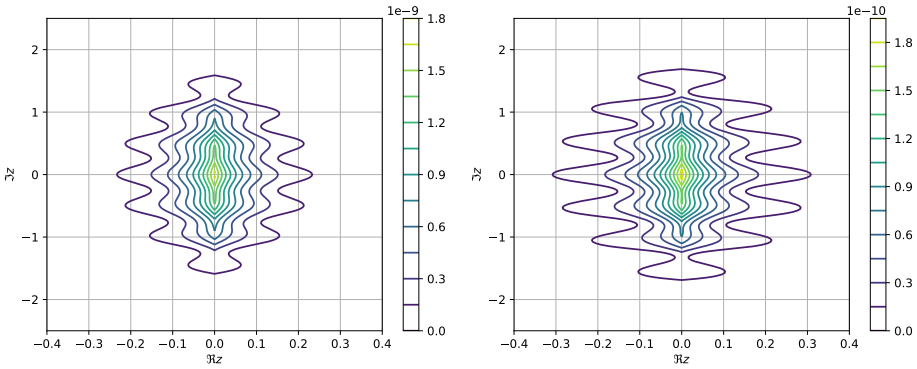

Fig. 6 Magnitude of the error computing $E_{1/2}(z)$ for a quadrature rule with $N = 10$ using parabolic (left) and hyperbolic (right) contours.

and

$$\psi_{2,\alpha}(\varepsilon) = \frac{(1+\varepsilon)^\alpha - (1+\alpha\varepsilon)}{\varepsilon^2} = \sum_{k=2}^{\infty} \binom{\alpha}{k} \varepsilon^{k-2} \tag{29}$$

for $|\varepsilon| < 1$. The functions $\psi_{1,\alpha}$ and $\psi_{2,\alpha}$ may be evaluated to high accuracy when $|\varepsilon|$ is small by suitable truncation of these Taylor expansions or by employing the library functions `expm1` and `log1p`. Since $w^\alpha - z = z\varepsilon\psi_{1,\alpha}(\varepsilon) = z\varepsilon[\alpha + \varepsilon\psi_{2,\alpha}(\varepsilon)]$ we find that

$$f_1(w;z) = \frac{\psi_{1,\alpha-\beta}(\varepsilon) - \alpha^{-1}\psi_{2,\alpha}(\varepsilon)}{\gamma^\beta \psi_{1,\alpha}(\varepsilon)} \quad \text{with} \quad f_1(\gamma;z) = \frac{1+\alpha-2\beta}{2\alpha\gamma^\beta}.$$

Summarizing: for $0 < \alpha < 1$, the Mittag-Leffler function $E_{\alpha,\beta}(z)$ is approximated by

$$E_{\alpha,\beta,N}(z) = \begin{cases} Q_{\star,N}(f;z) & \text{if } \alpha\pi < |\arg z| \le \pi, \\ \alpha^{-1} z^{(1-\beta)/\alpha} \exp(z^{1/\alpha}) + Q_{\star,N}(f_1;z) & \text{if } |\arg z| \le \alpha\pi. \end{cases} \tag{30}$$

We will use superscripts "par" and "hyp" to distinguish between the parabolic and hyperbolic cases where needed, so that

$$E_{\alpha,\beta}(z) = E^{\text{par}}_{\alpha,\beta,N}(z) + O(8.12^{-N}) \quad \text{and} \quad E_{\alpha,\beta}(z) = E^{\text{hyp}}_{\alpha,\beta,N}(z) + O(10.13^{-N}). \tag{31}$$

Example 3.1 We used both types of contour to compute $E_{1/2}(z)$ with $N = 10$ and obtained for the errors the patterns shown in Fig. 6. As expected, the hyperbolic contour gave somewhat more accurate results, with the error everywhere smaller than $1{\cdot}9 \times 10^{-10}$, compared to $1{\cdot}7 \times 10^{-9}$ for the parabolic contour. In both cases, the error is concentrated near the origin. At the origin itself, the computed value of $E_\alpha(0+i0)$ is `NaN` due to the factor $z^{(1-\beta)/\alpha} = (0+i0)^{(0+i0)}$ in (30).

Remark 3.3 When z is close to zero, it is usually best to compute $E_{\alpha,\beta}(z)$ by truncating its Taylor expansion (3). In particular, for $\beta > 1$ the factor $z^{(1-\beta)/\alpha}$ in (30) blows up as $z \to 0$.

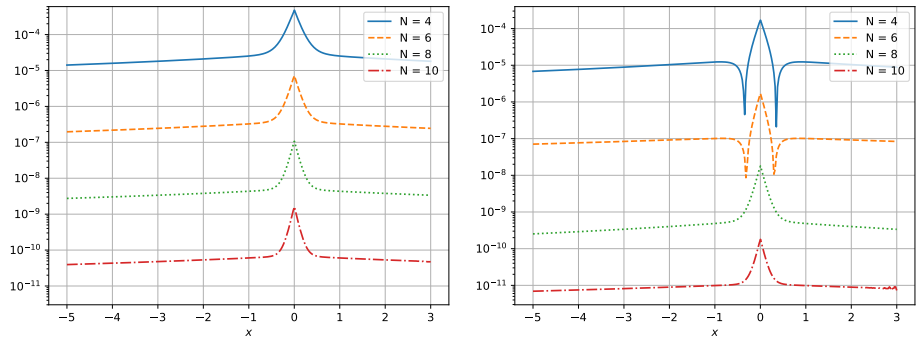

Fig. 7 The absolute error $|E_{1/2,1}(-x) - E_{1/2,1,N}(-x)|$ for increasing choices of N, using parabolic (left) and hyperbolic (right) contours.

4 Evaluation on the real line

For z on the real line, the functions from (13) and (26) satisfy

$$f(\bar{w};x) = \overline{f(w;x)} \quad \text{and} \quad f_1(\bar{w};x) = \overline{f_1(w;x)} \quad \text{for } u, x \in \mathbb{R},$$

so it follows using the properties (22) of the quadrature points and coefficients that we can nearly halve the number of function evaluations required to approximate the contour integral because

$$Q_{\star,N}(f;x) = A\left(C_0 f\big(w(0);x\big) + 2\sum_{n=1}^{N} \Re\big[C_n f\big(w(nh_\star);x\big)\big]\right).$$

Assume $0 < \alpha < 1$ and $x > 0$. Taking $z = -x$ we have $\theta = \pi$ so

$$E_{\alpha,\beta,N}(-x) = Q_{\star,N}(f;-x). \tag{32}$$

However, taking $z = x$ means that $\theta = 0$ and $\gamma = x^{1/\alpha}$, so

$$E_{\alpha,\beta,N}(x) = \alpha^{-1} x^{(1-\beta)/\alpha} \exp(x^{1/\alpha}) + Q_{\star,N}(f_1;x). \tag{33}$$

In fact, (33) is valid for $0 < \alpha < 2$ because $w = x^{1/\alpha}$ is still the only solution to $w^\alpha - x = 0$ with $|\arg w| \le \pi$.

Example 4.1 Figure 7 shows the absolute errors in $E_{1/2,1,N}(x)$ for $-5 \le x \le 3$ on a log scale. The convergence behaviour is consistent with the predictions (31) from the analysis above. Similar calculations reveal that the accuracy does not vary much with respect to $\alpha \in (0,1]$. As observed earlier in Fig. 6 the maximum error occurs at $x = 0$, and since $f(w;0) = w^{-\beta}$ and $E_{\alpha,\beta}(0) = 1/\Gamma(\beta)$ are independent of α, the difference $Q_{\star,N}(f;0) - 1/\Gamma(\beta)$ provides a readily computable measure of the expected accuracy of $E_{\alpha,\beta,N}(-x)$ for $x > 0$ and $0 < \alpha \le 1$. On the positive half-line, we find that as x increases from 0 the computed value $E_{\alpha,\beta,N}(x)$ is quickly dominated by the first term in (33). For instance, $E_{1/2}(3) \approx 2\exp(3^2) \doteq 16{,}206$.

Suppose now that $1 < \alpha < 2$, $z = -x$ and $x > 0$. The equation $w^\alpha + x = 0$ then has two solutions $w = \gamma_\pm = x^{1/\alpha}\exp(\pm i\pi/\alpha)$ satisfying

$$-\pi < \arg\gamma_- < -\frac{\pi}{2} \quad \text{and} \quad \frac{\pi}{2} < \arg\gamma_+ < \pi.$$

As an alternative to applying the identity (12) we can deal with the singularities $\gamma_\pm$ using a similar, albeit more complicated, approach to the one that led to (33). Write

$$\frac{1}{w^\alpha+x}=\varphi(w;x)\left(\frac{1}{w-\gamma_+}+\frac{1}{w-\gamma_-}\right),$$

where the function

$$\varphi(w;x)=\frac{(w-\gamma_+)(w-\gamma_-)}{(w^\alpha+x)(2w-\gamma_+-\gamma_-)}$$

has removable singularities at $w=\gamma_\pm$ with $\varphi(\gamma_\pm;x)=\alpha^{-1}\gamma_\pm^{1-\alpha}$. Define

$$f_\pm(w;x)=\frac{w^{\alpha-\beta}\varphi(w;x)-\gamma_\pm^{\alpha-\beta}\varphi(\gamma_\pm;x)}{w-\gamma_\pm}=\frac{w^{\alpha-\beta}(w-\gamma_\mp)}{(w^\alpha+x)(2w-\gamma_+-\gamma_-)}-\frac{\alpha^{-1}\gamma_\pm^{1-\beta}}{w-\gamma_\pm}$$

so that

$$w^{\alpha-\beta}\,\frac{\varphi(w;x)}{w-\gamma_\pm}=\frac{\alpha^{-1}\gamma_\pm^{1-\beta}}{w-\gamma_\pm}+f_\pm(w;x).$$

In this way, letting $f_2(w;x)=f_+(w;x)+f_-(w;x)$, it follows that

$$f(w;-x)=\frac{w^{\alpha-\beta}}{w^\alpha+x}=\frac{1}{\alpha}\left(\frac{\gamma_+^{1-\beta}}{w-\gamma_+}+\frac{\gamma_-^{1-\beta}}{w-\gamma_-}\right)+f_2(w;x).$$

Putting $z=-x$ in the integral representation (5), we see that

$$E_{\alpha,\beta}(-x)=\frac{1}{\alpha}\left(\gamma_+^{1-\beta}e^{\gamma_+}+\gamma_-^{1-\beta}e^{\gamma_-}\right)+\frac{1}{2\pi i}\int_{\mathscr{C}}e^w f_2(w;x)\,dw, \tag{34}$$

with $f_2(w;x)$ analytic for all w in the cut plane and satisfying $f_2(\bar{w};x)=\overline{f_2(w;x)}$, and with

$$\gamma_+^{1-\beta}e^{\gamma_+}+\gamma_-^{1-\beta}e^{\gamma_-}=2x^{(1-\beta)/\alpha}\exp\left(x^{1/\alpha}\cos\frac{\pi}{\alpha}\right)\cos\left((1-\beta)\frac{\pi}{\alpha}+x^{1/\alpha}\sin\frac{\pi}{\alpha}\right). \tag{35}$$

To compute $f_\pm(w;x)$ for w close to $\gamma_\pm$, we let $\varepsilon_\pm=\frac{w-\gamma_\pm}{\gamma_\pm}$ so that

$$w=\gamma_\pm(1+\varepsilon_\pm),\quad w-\gamma_\pm=\gamma_\pm\varepsilon_\pm,\quad 2w-\gamma_\pm-\gamma_\mp=w-\gamma_\mp+\varepsilon_\pm\gamma_\pm,$$

and

$$w^\alpha+x=\gamma_\pm^\alpha\varepsilon_\pm\psi_{1,\alpha}(\varepsilon_\pm)=\gamma_\pm^\alpha\varepsilon_\pm\big[\alpha+\varepsilon_\pm\psi_{2,\alpha}(\varepsilon_\pm)\big].$$

We find that

$$f_\pm(w;x)=\frac{(w-\gamma_\mp)[\psi_{1,\alpha-\beta}(\varepsilon_\pm)-\alpha^{-1}\psi_{2,\alpha}(\varepsilon_\pm)]-\gamma_\pm\alpha^{-1}\psi_{1,\alpha}(\varepsilon_\pm)}{\gamma_\pm^\beta\psi_{1,\alpha}(\varepsilon_\pm)(w-\gamma_\mp+\varepsilon_\pm\gamma_\pm)},$$

and in particular,

$$f_\pm(\gamma_\pm;x)=\frac{(1+\alpha-2\beta)(\gamma_\pm-\gamma_\mp)-2\gamma_\pm}{2\alpha\gamma_\pm^\beta(\gamma_\pm-\gamma_\mp)}.$$

Similarly,

$$f_\mp(w;x)=\frac{\gamma_\pm^{1-\beta}(1+\varepsilon_\pm)^{\alpha-\beta}}{\psi_{1,\alpha}(\varepsilon)(w-\gamma_\mp+\varepsilon_\pm\gamma_\pm)}-\frac{\alpha^{-1}\gamma_\mp^{1-\beta}}{w-\gamma_\mp},$$

and in particular,

$$f_\mp(\gamma_\pm;x)=\frac{\gamma_\pm^{1-\beta}-\gamma_\mp^{1-\beta}}{\alpha(\gamma_\pm-\gamma_\mp)}=x^{-\beta/\alpha}\,\frac{\sin\pi(1-\beta)/\alpha}{\alpha\sin\pi/\alpha}.$$

5 Approximations of Padé type

For $0 < \alpha \le 1$, consider the problem of approximating $E_{\alpha,\beta}(-x)$ by a rational function $p(x)/q(x)$ where

$$p(x) = \sum_{j=0}^{r} p_j x^j \quad \text{and} \quad q(x) = \sum_{j=0}^{r} q_j x^j.$$

Zeng and Chen [21] proposed a two-point Padé scheme, with the coefficients determined by the conditions

$$E_{\alpha,\beta}(-x) = \frac{p(x)}{q(x)} + \begin{cases} O(x^m) & \text{as } x \to 0, \\ O(x^{-n}) & \text{as } x \to \infty, \end{cases} \tag{36}$$

with appropriate choices of m and n. They obtained closed-form expressions for p_j and q_j in terms of α and β for some small choices of r. Let

$$a(x) = \sum_{k=0}^{m-1} a_k x^k \quad \text{and} \quad b(x) = \sum_{k=1}^{n-1} b_k x^k,$$

where, recalling (11),

$$a_k = \frac{(-1)^k}{\Gamma(\beta + k\alpha)} \quad \text{and} \quad b_k = \frac{(-1)^{k-1}}{\Gamma(\beta - k\alpha)} = \frac{(-1)^k}{\pi} \sin \pi(k\alpha - \beta)\Gamma(1 + k\alpha - \beta).$$

With the above definitions, (1) and (10) imply that

$$E_{\alpha,\beta}(-x) = \begin{cases} a(x) + O(x^m) & \text{as } x \to 0, \\ b(x^{-1}) + O(x^{-n}) & \text{as } x \to \infty, \end{cases}$$

so the conditions in (36) hold iff

$$\frac{p(x)}{q(x)} - a(x) = O(x^m) \quad \text{as } x \to 0,$$

and

$$\frac{x^{-r}p(x)}{x^{-r}q(x)} - b(x^{-1}) = O(x^{-n}) \quad \text{as } x \to \infty,$$

or equivalently, assuming $q_0 \ne 0$,

$$p(x) - a(x)q(x) = O(x^m) \quad \text{as } x \to 0, \tag{37}$$

and, assuming $q_r \ne 0$,

$$x^{-r}\big[p(x) - b(x^{-1})q(x)\big] = O(x^{-n}) \quad \text{as } x \to \infty. \tag{38}$$

Setting the coefficient of x^k on the left-hand side of (37) to zero for $0 \le k \le m-1$, and the coefficient of x^{-k} on the left-hand side of (38) to zero for $0 \le k \le n-1$, provides us with $m+n$ equations for the $2(r+1)$ unknown coefficients of the polynomials p and q. However, since the ratio p/q is unchanged if the numerator and denominator are multiplied by a common non-zero factor, we are free to impose a scaling condition that reduces the number of degrees of freedom to $2r+1$, suggesting that we should require

$$m + n = 2r + 1.$$

Furthermore, since $b(0) = 0$, the left-hand side of (38) equals $p_r + O(x^{-1})$ so we must have $p_r = 0$.

If $m \geq r+1$, then $n = 2r+1-m \leq r$ and we find that

$$\begin{aligned} p_k - \sum_{j=0}^{k} a_{k-j} q_j &= 0 \quad \text{for } 0 \leq k \leq r-1, \\ -\sum_{j=0}^{r} a_{k-j} q_j &= 0 \quad \text{for } r \leq k \leq m-1, \\ p_k - \sum_{j=k+1}^{r} b_{j-k} q_j &= 0 \quad \text{for } r-n+1 \leq k \leq r-1, \end{aligned}$$

whereas if $m \leq r$, then $n = 2r+1-m \geq r+1$ and

$$\begin{aligned} p_k - \sum_{j=0}^{k} a_{k-j} q_j &= 0 \quad \text{for } 0 \leq k \leq m-1, \\ -\sum_{j=0}^{r} b_{j-k} q_j &= 0 \quad \text{for } -(r-m) \leq k \leq -1, \\ p_k - \sum_{j=k+1}^{r} b_{j-k} q_j &= 0 \quad \text{for } 0 \leq k \leq r-1. \end{aligned}$$

In either case, we obtain a $(2r) \times (2r+1)$ homogeneous linear system of the form

$$C\mathbf{x} = 0 \quad \text{where} \quad \mathbf{x} = [p_0, p_1, \ldots, p_{r-1}, q_0, q_1, \ldots, q_r]^\top.$$

If the matrix C has full rank, then x must belong to a one-dimensional subspace of $\mathbb{R}^{2r+1}$.

Let $\mathbf{c}_j$ denote the jth column of C. Following Zeng and Chen [21] we can fix a solution by putting $x_{r+1} = q_0 = 1$ to obtain a $(2r) \times (2r)$ linear system

$$\tilde{C}\tilde{\mathbf{x}} = -\mathbf{c}_{r+1}$$

where $\tilde{C} = [\mathbf{c}_1, \ldots, \mathbf{c}_r, \mathbf{c}_{r+2}, \ldots, \mathbf{c}_{2r+1}]$ and $\tilde{\mathbf{x}} = [p_0, \ldots, p_{r-1}, q_1, \ldots, q_r]^\top$. This linear system is badly conditioned, the more so the smaller the value of α and the larger the value of r, but in practice we observe an autocorrection phenomenon [8,10] so that the computed values of $p(x)/q(x)$ can nevertheless provide an accurate approximation to $E_{\alpha,\beta}(-x)$.

In fact, computing the singular-value decomposition (SVD),

$$\tilde{C} = \tilde{U}\tilde{S}\tilde{V}^\top, \quad \tilde{S} = \operatorname{diag}(\tilde{\sigma}_1, \tilde{\sigma}_2, \ldots, \tilde{\sigma}_{2r}), \quad \tilde{\sigma}_1 \geq \tilde{\sigma}_2 \geq \cdots \geq \tilde{\sigma}_{2r},$$

so that $\tilde{S}(\tilde{V}^\top \tilde{\mathbf{x}}) = -\tilde{U}^\top \mathbf{c}_{r+1}$, we find that the last few singular values become very small but so do the corresponding components of $\tilde{U}^\top \mathbf{c}_{r+1}$. Thus, the computed coefficients in the solution vector $\tilde{\mathbf{x}}$ are of moderate size.

Instead of fixing $q_0 = 1$, we can compute the SVD of the whole $(2r) \times (2r+1)$ matrix, $C = USV^T$. Here, the diagonal matrix S is $(2r) \times (2r+1)$, and hence the orthogonal matrices U and V are $(2r) \times (2r)$ and $(2r+1) \times (2r+1)$, respectively. Let $\mathbf{e}_j$ denote the jth standard basis vector in $\mathbb{R}^{2r+1}$ and put

$$\mathbf{x} = V\mathbf{e}_{2r+1} = \text{last column of } V,$$

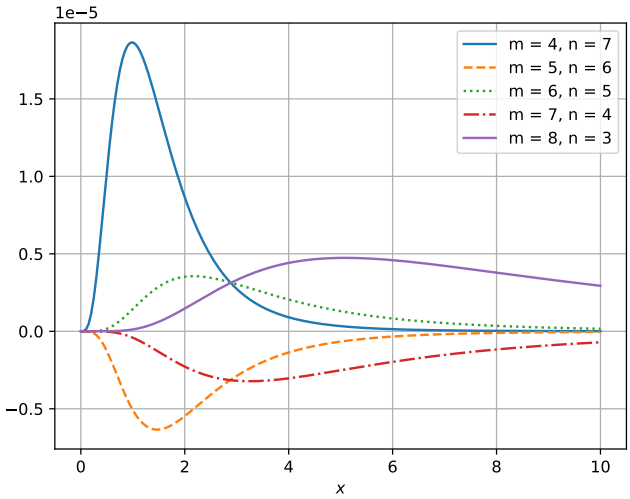

Fig. 8 The error $p(x)/q(x) - E_{1/2}(-x)$ for different choices of m and n with $r = 5$.

so that $V^\top \mathbf{x} = \mathbf{e}_{2r+1}$. It follows that $C\mathbf{x} = USV^T\mathbf{x} = US\mathbf{e}_{2r+1} = \mathbf{0}$ because the last column of S is zero. Since V is orthogonal, this choice of $\mathbf{x}$ results in the normalization

$$\sum_{j=0}^{r-1} p_j^2 + \sum_{j=0}^{r} q_j^2 = 1.$$

Having computed $p(x)/q(x)$ in this way, if desired we can of course rescale the coefficients so that $q(0) = q_0 = 1$.

A third option is to compute the LU factorization of C with partial pivoting, $C = PLU$, and solve the $(2r) \times (2r+1)$, homogeneous, upper triangular system $U\mathbf{x} = \mathbf{0}$ by setting $x_{2r+1} = q_r = 1$ and using back substitution. Provided $x_r = q_0 \neq 0$, the coefficients can again be rescaled so that $q_0 = 1$, if desired. However, we found that C and U are nearly as badly conditioned as $\tilde{C}$. For example, with $\alpha = 0.2$, $\beta = 1$, $m = 9$ and $n = 8$ the condition numbers of $\tilde{C}$, C and U are about $1{\cdot}39 \times 10^{13}$, $4{\cdot}83 \times 10^{12}$ and $1{\cdot}70 \times 10^{12}$, respectively, with the coefficients p_j and q_j in agreement to only about 4 significant figures. Nevertheless, the values of $p(x)/q(x)$ computed using these three approaches agree to within about 6×10^{-16} for $0 \le x < \infty$.

Example 5.1 Figure 8 shows the error in the Padé approximation of $E_{1/2}(-x)$ for five choices of m and n such that $m + n = 11$. Not surprisingly, increasing m improves the accuracy for small x at the expense of worse accuracy for large x. Increasing n has the opposite effect, and the accuracy for middling values of x is best when m and n are roughly equal. Figure 9 plots the absolute error when $m = r + 1$ and $n = r$, showing how the accuracy improves with increasing values of r.

Example 5.2 Figure 10 illustrates how the accuracy of the Padé approximation gets worse as α increases while keeping m and n fixed; in this case, $m = 6$ and $n = 5$.

Let $\chi_1, \chi_2, \ldots, \chi_r$ denote the zeros of q, so that $q(z) = q_r \prod_{j=1}^{r} (z - \chi_j)$, and assume for simplicity that the roots are distinct. For z in some neighbourhood of the negative real axis,

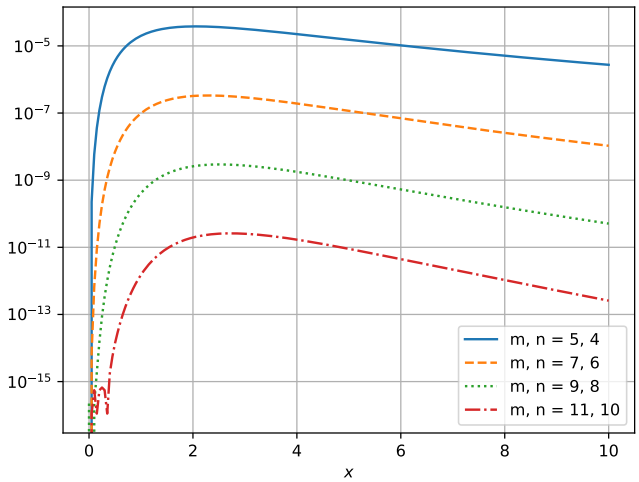

Fig. 9 The absolute error $|E_{1/2}(-x) - p(x)/q(x)|$ when $m = r+1$ and $n = r$ for increasing choices of r.

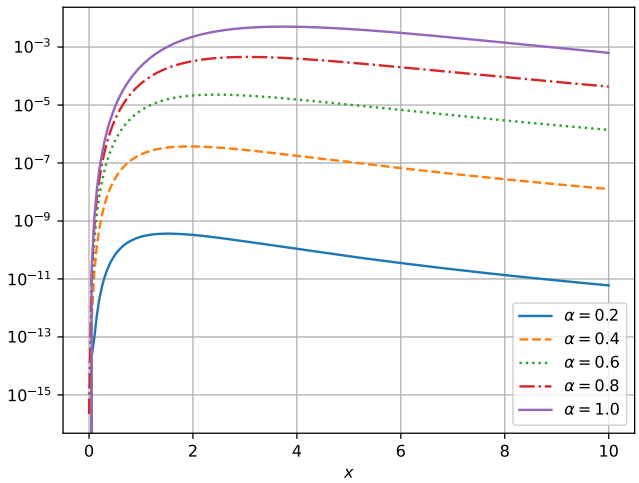

Fig. 10 The absolute error $|p(x)/q(x) - E_\alpha(-x)|$ for different choices of α with fixed polynomial degrees $m = 6$ and $n = 5$.

consider the partial fraction expansion

$$E_{\alpha,\beta}(z) \approx \frac{p(-z)}{q(-z)} = \sum_{j=1}^{r} \frac{\rho_j}{z+\chi_j} \quad \text{where} \quad \rho_j = -\frac{p(\chi_j)}{q'(\chi_j)}.$$

We can compare this rational approximation with the one discussed in Remark 3.2.

Example 5.3 Figure 11 shows contour plots of the base-10 logarithm of the absolute error for the two types of rational approximation to $E_{1/2}(z)$ for $-5 \le \Re z \le 3$ and $-4 \le \Im z \le 4$, with the locations of the poles shown as red dots. The quadrature approximation using a hyperbola for $N = 5$ is compared with the Padé approximation for $m = 12$ and $n = 11$, so that

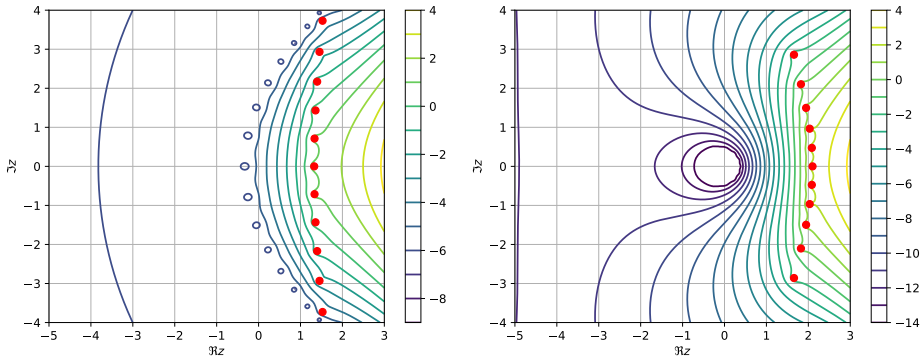

Fig. 11 Contour plots of $\log_{10}|E_{1/2}(z) - Q^{\mathrm{hyp}}_{\star,N}(f;z)|$ (left) for $N = 5$ and $\log_{10}|E_{1/2}(z) - p(-z)/q(-z)|$ (right) for $m = 6$ and $n = 5$. The red dots mark the locations of the 11 poles for each of the rational approximations.

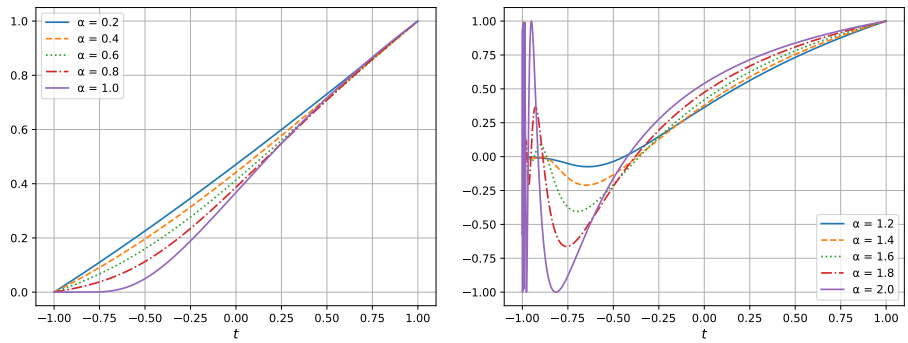

Fig. 12 The function $f_\alpha(t)$ correponding to $E_\alpha(-x)$ under the change of variable (39), for values of α in the range $0 < \alpha \le 1$ (left) and $1 < \alpha \le 2$ (right).

both sums have $r = 2N+1 = 11$ terms. Recall from (10) that $E_{1/2}(z) = 2\exp(z^2) + O(z^{-1})$ as $|z| \to \infty$ when $|\arg z| \le \pi/2$, so we cannot expect either approximation to work for $\Re z > 0$, except near $z = 0$. However, both are effective for $\Re z < 0$. In this case, the Padé approximation $p(-z)/q(-z)$ achieves higher accuracy than the quadrature approximation $Q^{\mathrm{hyp}}_{\star,N}(z)$.

6 Best approximation by rational functions

For a real interval I, let $\mathscr{R}^m_n(I)$ denote the set of rational functions p/q where $p : I \to \mathbb{R}$ and $q : I \to \mathbb{R}$ are polynomials of degree at most m and n, respectively. In light of the preceding results, it is natural to ask what is the best possible accuracy achievable when approximating $E_\alpha(-x)$ for $0 \le x < \infty$ by a function in $\mathscr{R}^m_n\big([0,\infty)\big)$. For $\alpha = 1$, that is, for the exponential function e^{-x}, and for $m = n$, this question was addressed by Nakatsukasa et al. [14, Section 6.8] and we will adapt their approach.

The substitution

$$x = G(t) = \frac{1-t}{1+t} \quad \text{for } -1 \le t \le 1 \tag{39}$$

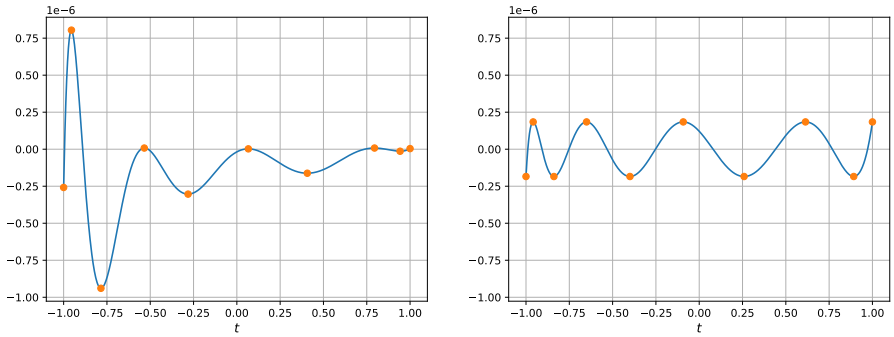

Fig. 13 Errors in rational approximations from $\mathscr{R}_m^m$ to $f_{1/2}(t) = E_{1/2}(-x)$ for $m = 4$: (left) by the AAA algorithm and (right) following subsequent iterations of the Remez algorithm. The local extrema are marked with dots.

Table 2 The uniform error $\|f_\alpha - R\|_{L_\infty(-1,1)}$ in the rational function $R \in \mathscr{R}_m^m$ generated by the AAA algorithm.

m	$\alpha = 0{\cdot}2$	$\alpha = 0{\cdot}4$	$\alpha = 0{\cdot}6$	$\alpha = 0{\cdot}8$	$\alpha = 1{\cdot}0$
1	9.94e-01	9.94e-01	9.94e-01	9.94e-01	9.95e-01
2	3.12e-03	1.30e-02	3.11e-02	6.13e-02	1.01e-01
3	2.52e-05	4.27e-04	2.35e-03	8.29e-03	2.10e-02
4	7.19e-08	4.29e-06	4.45e-05	3.45e-04	3.72e-03
5	2.86e-10	1.25e-07	5.05e-06	5.78e-05	3.12e-04
6	1.76e-12	1.10e-09	9.90e-08	2.74e-06	6.28e-05
7	1.45e-14	4.69e-11	4.91e-09	1.49e-07	2.71e-06
8	6.34e-13	4.61e-13	1.30e-10	7.84e-09	3.04e-07
9	1.28e-12	1.53e-14	8.86e-12	1.66e-09	7.11e-08
10	4.30e-13	1.90e-11	1.83e-13	5.49e-11	5.17e-09

defines a one-one mapping $G : [-1,1] \to [0,\infty]$ with inverse given by

$$t = G^{-1}(x) = \frac{1-x}{1+x} \quad \text{for } 0 \le x \le \infty,$$

if we agree that $G(-1) = \infty$. Also, G induces a bijection $\mathscr{R}_m^m\big((-\infty,0]\big) \to \mathscr{R}_m^m\big((-1,1]\big)$ given by $f \mapsto f_\sharp$, where $f_\sharp(t) = f\big(-G(t)\big)$. Thus, it suffices to find the best approximation from $\mathscr{R}_m^m([-1,1])$ to the function $f_\alpha = (E_\alpha)_\sharp$, or in other words, the function

$$f_\alpha(t) = E_\alpha\big(-x\big). \tag{40}$$

Figure 12 plots f_α for selected values of α in the range $0 < \alpha \le 2$. Recall from (2) that $E_0(-x) = 1/(1+x)$ is already a rational function in $\mathscr{R}_1^0 \subseteq \mathscr{R}_1^1$. If $0 < \alpha \le 1$, then f_α is well behaved and we can hope to approximate it accurately by a function in $\mathscr{R}_m^m([-1,1])$ with moderate values of m. However, such an approximation becomes less and less feasible as $\alpha > 1$ increases because $f_\alpha(t)$ oscillates rapidly near $t = -1$ due to the cosine factor in the term (35).

For $0 < \alpha \le 1$, we applied the adaptive Antoulas–Anderson (AAA) algorithm [14] to generate an initial approximation $f_\alpha \approx R \in \mathscr{R}_m^m([-1,1])$, and computed the local extrema

Table 3 The uniform error $\|f_\alpha - R^*\|_{L_\infty(-1,1)}$ in the best rational approximation $R^* \in \mathscr{R}_m^m$.

m	$\alpha = 0{\cdot}2$	$\alpha = 0{\cdot}4$	$\alpha = 0{\cdot}6$	$\alpha = 0{\cdot}8$	$\alpha = 1{\cdot}0$
1	5.00e-01	5.00e-01	5.00e-01	5.00e-01	5.00e-01
2	2.08e-03	8.55e-03	2.02e-02	3.87e-02	6.68e-02
3	7.72e-06	1.30e-04	7.13e-04	2.55e-03	7.36e-03
4	2.83e-08	1.94e-06	2.48e-05	1.66e-04	7.99e-04
5	1.04e-10	2.89e-08	8.61e-07	1.07e-05	8.65e-05
6	3.80e-13	4.31e-10	2.98e-08	6.93e-07	9.35e-06
7		6.41e-12	1.03e-09	4.47e-08	1.01e-06
8			3.56e-11	2.89e-09	1.09e-07
9			1.23e-12	1.35e-09	1.17e-08
10				1.20e-11	1.26e-09

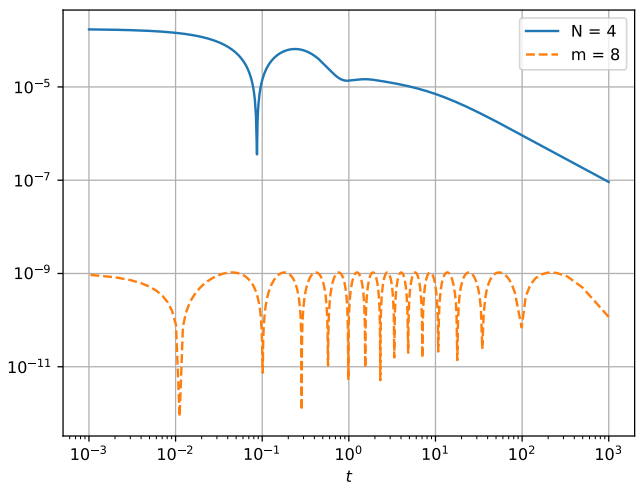

Fig. 14 Solid line: the absolute error in the rational approximation $E_{\alpha,\beta}(-x) \approx Q_{\star,N}^{\mathrm{hyp}}(-x)$ from $\mathscr{R}_{2N+1}^{2N}\big([0,\infty)\big)$ when $\alpha = 0{\cdot}75$, $\beta = 1$ and $N = 4$. Dashed line: the absolute error in the best approximation from $\mathscr{R}_m^m\big([0,\infty)\big)$ for $m = 2N = 8$.

$-1 \le t_0 < t_1 < \cdots < t_{2m+1} \le 1$ of the error $f_\alpha - R$. These points where then used to initialise a rational Remez algorithm [1] that generated the minimax approximation $R^* \in \mathscr{R}_m^m([-1,1])$, which minimizes the error in the uniform norm and is characterized by the equioscillation property

$$f_\alpha(t_l^*) - R^*(t_l^*) = (-1)^{l+1}\lambda \quad \text{for } 0 \le l \le 2m+1,$$

where t_0^*, t_1^*, …, t_{2m+1}^* are the local extrema of $f_\alpha - R^*$ and so $|\lambda| = \|f_\alpha - R^*\|_{L_\infty(-1,1)}$. Figure 13 shows the errors in these approximations when $\alpha = 1/2$ and $m = 4$. In Tables 2 and 3, we see how the uniform errors in R and R^* tend to zero as the polynomial degree m increases. The convergence is most rapid for smaller values of α, as might be expected from the behaviour of f_α seen in Fig. 12. The effects of roundoff become apparent once the errors reach about 10^{-13}, and the missing entries of Table 3 are cases when the Remez algorithm failed. When computing R and R^*, we evaluated $f_\alpha(t) = E_\alpha(-x)$ using the method of Section 4 with $N = 14$ and hyperbolic contours.

Finally, recall from Remark 3.2 that the quadrature method generates a rational approximation $E_{\alpha,\beta}(-x) \approx Q_{\star,N}(f;-x)$ from $\mathscr{R}^{2N}_{2N+1}\big([0,\infty)\big)$ when $0<\alpha<1$. Fig. 14 compares the absolute error using this approximation with that of the best approximation from $\mathscr{R}^{m}_{m}\big([0,\infty)\big)$ when $m=2N$ in the case $\alpha = 0{\cdot}6$, $\beta = 1$ and $N=4$. The latter is smaller by 2 to 5 orders of magnitude.

7 Conclusion

The quadrature-based approach of Section 3 provides a practical method for numerical evaluation of the Mittag-Leffler function $E_{\alpha,\beta}(z)$. The maximum error can be reduced to around 10^{-N} using about N terms, up to around $N=14$ when using standard 64-bit floating-point arithmetic; higher accuracy is achievable with larger N if extended precision is used. Somewhat better efficiency is possible for sufficiently small $|z|$ using just the Taylor expansion (1), and for sufficiently large $|z|$ using the asymptotic expansion (10). In the practically-important case when $0<\alpha<1$, rational approximation of $E_{\alpha,\beta}(-x)$ for $0 \le x < \infty$ is effective.

References

1. Filip, S.I., Nakatsukasa, Y., Trefethen, L.N., Beckermann, B.: Rational minimax approximation via adaptive barycentric representations. SIAM J. Sci. Comput. **40**(4), A2427–2455 (2018). DOI 10.1137/17M1132409
2. Garrappa, R.: Numerical evaluation of two and three parameter Mittag-Leffler functions. SIAM J. Numer. Anal. **53**(3), 1350–1369 (2015). DOI 10.1137/140971191
3. Garrappa, R., Poplizio, M.: Evaluation of generalized Mittag-Leffler functions on the real line. Adv. Comput. Math. **39**, 205–225 (2013). DOI doi.org/10.1007/s10444-012-9274-z
4. Gill, G., Straka, P.: MittagLeffleR: Using the Mittag-Leffler distributions in R (2017). URL `https://strakaps.github.io/MittagLeffleR/`
5. Gorenflo, R., Kilbas, A.A., Mainardi, F., Rogosin, S.V.: Mittag-Leffler Functions, Related Topics and Applications. Springer (2014). DOI 10.1007/978-3-662-43930-2
6. Gorenflo, R., Loutchko, J., Luchko, Y.: Computation of the Mittag-Leffler function $E_{\alpha,\beta}(z)$ and its derivative. Frac. Calc. Appl. Anal. **5**(4), 491–518 (2002). URL `http://www.diogenes.bg/fcaa/volume6/fcaa61/aluchcor54.pdf`
7. Haubold, H.J., Mathai, A.M., Saxena, R.K.: Mittag-Leffler functions and their applications. J. Appl. Math. **2011** (2011). DOI 10.1155/2011/298628
8. Litvinov, G.L.: Error autocorrection in rational approximation and interval estimates. [a survey of results.]. Centr. Eur. J. Math. **1**, 36–60 (2003). DOI 10.2478/BF02475663
9. López-Fernández, M., Palencia, C.: On the numerical inversion of the Laplace transform of certain holomorphic mappings. Appl. Numer. Math. **51**(2), 289–303 (2004). DOI 10.1016/j.apnum.2004.06.015
10. Luke, Y.L.: Computations of coefficients in the polynomials of Padé approximations by solving systems of linear equations. Journal of Computational and Applied Mathematics **6**(3), 213–218 (1980). DOI 10.1016/0771-050X(80)90028-5
11. McLean, W.: MittagLefflerFunctions. `https://github.com/billmclean/MittagLefflerFunctions.jl` (2020)
12. McNamee, J., Stenger, F., Whitney, E.L.: Whittaker's cardinal function in retrospect. Math. Comp. **25**(113) (1971). DOI 10.1090/S0025-5718-1971-0301428-0
13. Mittag-Leffler, G.M.: Une généralization de l'intégrale de Laplace–Abel. Comp. Rend. Acad. Sci. Paris **136**, 537–539 (1903)
14. Nakatsukasa, Y., Séte, O., Trefethen, L.N.: The AAA algorithm for rational approximation. SIAM J. Sci. Comput. **40**(3), A1494–A1522 (2018). DOI 10.1137/16M1106122
15. Paris, R.B.: Exponential asymptotics of the Mittag-Leffler function. Proc. Roy. Soc. Lond. A **458**, 3041–3052 (2002). DOI 10.2307/3560097
16. Paris, R.B.: Asymptotics of the Mittag-Leffler function $E_a(z)$ on the negative real axis when $a \to 1$. Arxiv preprint (2020). 2005.05737v1
17. Podlubny, I.: Mittag-Leffler function. URL `https://www.mathworks.com/matlabcentral/fileexchange/8738-mittag-leffler-function`. MATLAB Central File Exchange

18. Seybold, H., Hilfer, R.: Numerical algorithm for calculating the generalized Mittag-Leffler function. SIAM J. Numer. Anal. **47**(1), 69–88 (2008). DOI 10.1137/070700280
19. Weideman, J.A.C., Trefethen, L.N.: Parabolic and hyperbolic contours for computing the Bromwich integral. Math. Comp. **76**(259), 1341–1356 (2007). DOI 10.1090/S0025-5718-07-01945-X
20. Wong, R., Zhao, Y.Q.: Exponential asymptotics fo the Mittag-Leffler function. Constr. Approx. **18**, 355–385 (2002). DOI 10.1007/s00365-001-0019-3
21. Zeng, C., Chen, Y.Q.: Global Padé approximations of the generalized Mittag-Leffler function and its inverse. Frac. Calc. Appl. Anal. **18**, 1492–1506 (2015). DOI 10.1515/fca-2015-0086